Heliyon 10 (2024) e38074

Contents lists available at ScienceDirect

Heliyon

journal homepage: www.cell.com/heliyon

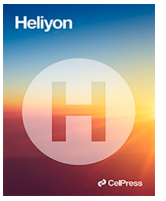

Research article

Therapeutic potential of *Leea asiatica*: Chemical isolation and validation of ethnomedicinal claims through *in vitro* and *in silico* assessment of antioxidant and anti-inflammatory properties

Khem Raj Joshi [a,b,*], Hari Prasad Devkota [a], Khalid Awadh Al-Mutairi [c], Koji Sugimura [a,**], Shoji Yahara [a], Ravindra Khadka [b], Shankar Thapa [d], Mohammad Ujair Shekh [b], Sandesh Poudel [b], Takashi Watanabe [a]

[a] *Graduate School of Pharmaceutical Sciences, Kumamoto University, 5-1 Oe-honmachi, Chuo-ku, Kumamoto, 862-0973, Japan*
[b] *School of Health and Allied Sciences, Faculty of Health Sciences, Pokhara University, Pokhara, 33700, Nepal*
[c] *University of Tabuk, Department of Biology, Faculty of Science, Tabuk, P.O. Box 741, Tabuk, 741, Saudi Arabia*
[d] *Department of Pharmacy, Madan Bhandari Academy of Health Sciences, Hetauda, Nepal*

A R T I C L E I N F O

Keywords:
Anti-inflammatory
In silico
Leea asiatica
TNF-α

A B S T R A C T

Leea asiatica (L.) Ridsdale has been used by different ethnic communities to manage diseased conditions that can be traced to oxidative stress and cellular inflammations but scientific evidences to support the claim are scanty. The objective of this study was to isolate and identify the antioxidants present in the aerial parts of *Leea asiatica,* perform their molecular docking against proteins to inspect whether the traditional uses of the plant can be validated by an in-silico approach. Quercetin (**1**), gallic acid (**2**), kaempferol (**3**), methyl gallate (**4**), myricetin 3-*O*-α-L-rhamnopyranoside (**5**), (−)-epicatechin-3-*O*-gallate (**6**) and (−)-epigallocatechin-3-*O*-gallate (**7**) were isolated from the 70 % methanolic extract of the aerial parts. Compounds **2**, **4**, **6**, and **7** are reported for the first time from *Leea asiatica*. Quercetin (**1**), gallic acid (**2**), (−)-epicatechin-3-*O*-gallate (**6**) and (−)-epigallocatechin-3-*O*-gallate (**7**) showed potent antioxidant activity against 1,1-diphenyl-2-picrylhydrazyl (DPPH) radical. Molecular docking with NADPH oxidase and TNF-α revealed that epicatechin-3-*O*-gallate, epigallocatechin-3-*O*-gallate and quercetin bound with the least binding energy amongst the isolated compounds as well as standard (Trolox and Prednisolone). By molecular dynamics analysis, epicatechin-3-*O*-gallate maintained stable conformation with NADPH oxidase and TNF-α and was found to possess good ADMET profile thereby validating the ethnic use of the plant as a medicine in the management of inflammatory conditions by an in vitro and *in silico* approach.

1. Introduction

Oxidants are vital for maintaining cellular redox balance, but an excess can lead to imbalance, with Reactive Oxygen Species (ROS) from aerobic respiration being particularly unstable and prone to causing oxidative damage to molecules and biomacromolecules [1,

* Corresponding author. School of Health and Allied Sciences, Faculty of Health Sciences, Pokhara University, Pokhara, 33700, Nepal.
** Corresponding author.
E-mail addresses: khemraj_pu@pu.edu.np (K.R. Joshi), sugimura@kumamoto-u.ac.jp (K. Sugimura).

https://doi.org/10.1016/j.heliyon.2024.e38074
Received 8 May 2024; Received in revised form 9 September 2024; Accepted 17 September 2024
Available online 18 September 2024

2]. Elevated oxidative stress is implicated in various chronic diseases, including diabetes, neurodegenerative conditions, cardiovascular issues, and cancer [3]. This stress triggers the activation of transcription factors, which, in turn, upregulate genes associated with growth factors and inflammatory cytokines, fostering pathways that can transform normal cells into cancerous ones [4]. Thus, antioxidants within the cells determine the cell's redox homeostasis and the mitigation of the stress caused by oxidants, especially when the initial defense mechanisms are overwhelmed [5]. During the metabolism of arachidonic acid, ROS are generated by different enzymes: NADPH oxidase, cytochrome P450 (CP450), Lipoxygenase (LO), Myeloperoxidase (MP), and Xanthine Oxidase (XO). Inhibition of such enzymes disrupts the ROS production cycle, reducing oxidative stress [6]. ROS mediated increase in oxidative stress can contribute to various diseases [7]. Consequently, the search for substances which can maintain redox balance (antioxidants) plays a pivotal role in discovering molecules that can cure, manage or prevent multiple diseases by mitigating oxidative stress [3–6].

Tumor necrosis factor (TNF-α) functions as a versatile pro-inflammatory cytokine, impacting immune cells significantly while also being pivotal in cellular processes of differentiation, proliferation, metabolism, inflammation, and cell death [8]. Tumor necrosis factor α (TNF-α) and tumor necrosis factor beta (TNF-β) are the two forms that have been identified. These variants exhibit structural and sequential similarities, vying for receptor binding in biological processes [9]. The functions of TNF-α are activated by their interactions with either of the two receptors: TNFR1 or p55 and TNFR2 or p75 (tumor necrosis factor receptor type I and tumor necrosis factor receptor type II respectively). The expression of TNFR2 typically occurs in immune cells, cells of the endothelia, and neurons under normal physiologies, while TNFR1 is ubiquitously expressed on nearly all nucleated cells, pivotal in initiating TNF-α signaling pathways [10]. After the binding of TNF-α to its receptors, it activates many pathways: extracellular signal regulated kinase (ERK), c-Jun N-terminal kinase, transcription factor NFκB mitogen activated protein kinase (MAPK) [11]. Physiologically, TNF-α crucially regulates immunological activities however, dysregulation of the activities of TNF-α has been associated to inflammatory conditions such as autoimmune diseases, cancer, and neurological illnesses [12]. Agents that antagonize TNF-α (Adalimumab, Certolizumab, Etanercept, Golimumab, and Infliximab) have transformed the treatment and management of inflammatory autoimmune disorders [13–17]. These medicines attach to the interface of TNF-α dimers and complexes, preventing TNF-α receptors from binding and activating downstream signaling pathways that cause inflammation. Drugs discovered thus far have higher molecular weight (proteins/antibodies) and are related with numerous side effects, such as TB, CHF, demyelinating illness, lupus, formation of autoantibodies, and systemic adverse effects [18–21]. The structure of dimeric TNF-α associated with SPD304 (a small inhibitor) was published in 2005 which revealed that TNF α's active site at the dimer interface is made up of sixteen amino acid contact residues. These are distributed in two chains, chain A with 9 amino acids and chain B with the remaining 7 amino acids. Of all the amino acids, the most important one is Tyr119. The chi-1 angles at Tyr119 rotate and form a dimer that facilitates chemical binding. When SPD304 interacts with key residues alteration occurs in trimer symmetry, causing monomer dissociation and stabilization of the dimer. This structure as the guide to create direct TNF-α suppressors by stabilizing its dimer structure in the form of small molecule inhibitors. There are currently no known orally active small molecule drugs against TNF-α. Identification of small compounds that can block the pathway regulated by TNF-α is a potential and current emphasis area [22].

The study of interactions between ligands and macromolecules is now possible with molecular docking. This technique provides insights into the regions of receptor activity, define which amino acids are involved during the interactions, and visualize the interaction of each atom of the ligand with the receptor (macromolecule) [23].

Leea asiatica Edgew. *(syn. Leea asiatica* Edgew, *Leea crispa* van Royen ex L, Family: Vitaceae*)* commonly known as Kumali/Guithe Padari in Nepal. It is a shrub, widely distributed in various parts of Asia, including Nepal, India, Bangladesh, Sri Lanka, Malaysia, and Thailand between 1300 and 2600m. The leaves and roots of *L. asiatica* are used traditionally to alleviate pain and inflammation [24]. Several studies report that the methanolic extracts of the plant possess analgesic, anti-inflammatory, hepatoprotective, and nephroprotective properties [25,26]. Studies focused on the characterization of phytoconstituents report the presence of flavonoids, phenolic glycosides, terpenoids, and several other secondary metabolites from the plant [27,28].

The current study focused on isolating and characterizing the major antioxidant constituents of *Leea asiatica* (aerial parts) and evaluating the potential of the isolates to inhibit NADPH oxidase and TNF-α by an *in silico* approach to validate the ethnobotanical use of the plant in different inflammatory disorders.

2. Materials and methods

2.1. Plant material

The fresh plant was collected from Lahachock, Kaski, Nepal in July 2014 and identified by Prof. Takashi Watanabe, Kumamoto University, Kumamoto, Japan. The voucher specimen (Voucher No.: KUNP20140825-9) was deposited at Graduate School of Pharmaceutical Sciences, Kumamoto University, Kumamoto, Japan.

2.2. Reagents, chemicals and equipment

TLC was performed on precoated silica gel 60 F_{254} plates (0.2 mm, aluminum sheet, Merck). 1,1-Diphenyl-2-picrylhydrazyl (DPPH) was obtained from Wako Pure Chemicals, Osaka, Japan, Trolox was used from Calbiochem (Denmark) and MES [2-(N-morpholino) ethane sulphonic acid] buffer was obtained from Dojindo Chemical Research, Kumamoto, Japan. Column chromatography (CC) was carried out with silica gel 60 (0.040–0.063 mm, Merck), MCI GEL® CHP20P (75–150 μm, Mitsubishi Chemical Industries Co., Ltd.), Sephadex® LH-20 (Amersham Pharmacia Biotech) and Chromatorex ODS (30–50 μm, Fuji Silysia Chemical Co., Ltd.). NMR spectra (^{1}H: 500 MHz and ^{13}C: 125 MHz) were measured and recorded as chemical shifts (ppm) with reference to TMS. Mass spectra were

recorded on JEOL JMS 700 MStation mass spectrometer.

2.3. Extraction and isolation of compounds from Leea asiatica aerial part

The shade dried aerial part of *L. asiatica* (1.8 kg) were extracted with 70 % MeOH (18 L x 2) at 50°C (5 h) and at room temperature (25°C, 19 h) to afford 204 g extract. The extract was suspended in water and fractionated with EtOAc. The aqueous fraction (116 g) was subjected on MCI GEL™ CHP20P column chromatography (CC) and eluted successively with water, 40 %, 60 %, 80 %, and 100 % MeOH to give five fractions (1–5). Fraction 1 (67 g, H2O eluate) was subjected on MCI GEL™ CHP20P CC to give three fractions (1-1∼1-3). Fraction 1–2 was subjected on Sephadex® LH-20 CC (50 % MeOH) to afford compound **2** (228 mg). Fraction 5 (2.74 g, 40 % MeOH eluate) was subjected on Sephadex® LH-20 CC (50 % MeOH) to afford compound **5** (329 mg) and compound **1** (23 mg). The EtOAc fraction (88 g) was suspended in MeOH and fractionated with n-hexane to obtain n-hexane and MeOH fractions. Then MeOH fraction (44 g) was subjected on MCI GEL™ CHP20P CC and eluted successively with 20 %, 40 %, 60 %, 80 %, and 100 % MeOH to give eleven fractions (1–11). Fraction 4 (3.66 g, 40 % MeOH eluate) was subjected successively on Sephadex® LH-20 CC (MeOH) and ODS (50%MeOH) to afford compound **6** (86 mg), **4** (33 mg), **7** (58 mg). Fraction 8 (1.10 g, 60 % MeOH eluate) was subjected on Sephadex® LH-20 CC (MeOH) to afford compound **1** (52 mg). Fraction 9 (4.17 g, 40 % MeOH eluate) was subjected on Sephadex® LH-20 CC (MeOH) to afford compound **3** (22 mg) (Fig. 1).

2.4. In vitro antioxidant activity

In vitro antioxidant activity was measured as the ability of the isolates to scavenge DPPH free radical using a microplate reader spectrophotometer [29]. For this, the compounds were made soluble in suitable solvents. 80 μL of sample and 40 μL of MES buffer (200 mM, pH 6.0) were mixed in a 96-well plate. 40 μL of DPPH solution (800 mM in EtOH) was then added to each of the wells. After shaking vigorously, the reaction mixture was allowed to stand for 30 min at room temperature protected from light. The anti-oxidant potency corresponding to the ability to scavenge DPPH radical was calculated by measuring the absorbance at 510 nm using a UV visible spectrophotometer using following formula:

$$\text{Radical scavenging activity (\%)} = 100 \times (A\text{-}B)/A$$

Where, A is the control absorbance of DPPH radicals' solution and B is the absorbance after incubating the reaction mixture. Trolox, the water-soluble analogue of vitamin E was used as the positive control and appropriate negative controls were used. Results are expressed as mean of four experiments. Effective Concentration (EC_{50}) value was calculated from a plot of concentration of samples vs % radical scavenging activity which is the concentration (μM) of the sample required for 50 % reduction of the DPPH radical absorbance.

2.5. Molecular docking study

Protein selection and preparations: Proteins: NADPH oxidase (PDB ID: 2CDU) for antioxidant activity and TNF- α (PDB ID:2AZ5) for anti-inflammatory activity, were selected based on the literature survey [3,5,12,22,30–32]. Protein models were downloaded from the protein data bank (https://www.rcsb.org/) in PDB format as target. 2CDU and 2AZ5 have better resolution (1.80 Å & 2.10 Å), no mutation, and the conformation were validated with Ramachandran plot (Supplementary Material Figs. S8 and S9). These protein models were prepared by eliminating heteroatoms, water molecules, cocrystal ligands and adding polar hydrogen via Discovery studio

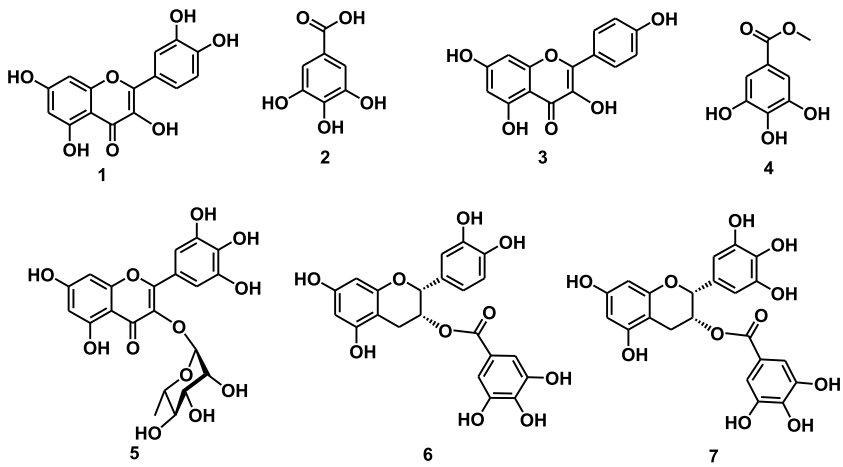

Fig. 1. Structures of compounds isolated from *Leea asiatica* aerial parts; quercetin (1), gallic acid (2), kaempferol (3), methyl gallate (4) myricetin 3-O-*α*-L-rhamnopyranoside (5), (−)-epicatechin-3-*O*-gallate (6) and (−)-epigallocatechin-3-*O*-gallate (7).

visualizer v24.1.0.23298 software and saved in PDB format for docking [33,34].

3D Ligand preparations: The 3D structure of 7 isolated compounds and standard drugs Trolox and Prednisolone were downloaded from PubChem database (https://pubchem.ncbi.nlm.nih.gov/) in '.sdf' format. These structures in. sdf format were optimized to minimum geometric configuration in PyRx 0.8 software and used for docking studies [35].

2.6. Ligand protein interactions

To perform the molecular docking, Autodock Vina wizard in PyRx 0.8. software was used [35,36]. Protein in PDB format was loaded in PyRx and converted to '.pdbqt' format through make macromolecule option. Open babel in PyRx was used to upload the 3D ligands and geometrical energy minimized to global energy minimum and converted to '.pdbqt' format [37]. The instance coordinates of co-crystallized ligand were downloaded in SDF format from protein data bank and interaction with the protein was visualized in Biovia Discovery studio to view interacting amino acids. The grid box parameter was set to cover all the interacting amino acids which are tabulated (Supplemental Material Table S13). We used default commands of software for docking and the best docked poses were visualized in BIOVIA Discovery studio [38–40].

2.7. Molecular docking simulation

To assess the stability of the most promising epicatechin-3-*O*-gallate in complex with the NADPH oxidase (PDB ID: 2CDU) and TNF-α (PDB ID:2AZ5) proteins, MD simulations (200 ns) were carried out using the OPLS3e force field within the Desmond package. This advanced computational approach provides insights into the dynamic behavior of the compound-enzyme complex over time, thereby allowing for a deeper understanding of the stability and interactions within the system. The simulation box parameters, solvation model, energy minimization, thermostat, and barostat methods used in this study were in line with those described in a previous study [41,42].

2.8. Prediction of ADMET properties, drug-likeness and medicinal chemistry

ADMET properties shows the absorption, distribution, metabolism, excretion, and toxicity of drugs. In the preclinical stages, it is a useful tool to predict the pharmacological and toxicological properties.

We used freely accessible SwissADME online web tool (http://www.swissadme.ch)to evaluate the pharmacokinetics, drug-likeness, and medicinal chemistry of the isolated molecules and standard drugs [43]. Similarly, we used another free webserver ProTox 3.0 (https://comptox.charite.de/protox3/) for the prediction of toxicity of isolated molecules and standards [44]. The compounds in SMILES format were downloaded from PubChem database (https://pubchem.ncbi.nlm.nih.gov/) and used for the prediction in both SwissADME and ProTox 3.0 web tools.

3. Results

3.1. Extraction, isolation and characterization

Maceration of the aerial parts (1.8 kg) of *L. asiatica* (shade dried) in 70 % MeOH (18 L x 2) at 50°C (5 h) and at room temperature (25°C, 19 h) gave 204 g of extract. The extract, suspended in water, was fractioned with ethyl acetate. Both water (116 g) and EtOAc (88 g) fraction were applied to separately in column chromatography (CC) on MCI GEL™ CHP20P, Sephadex® LH-20, ODS and silica gel to get compounds **1**–**7** (Fig. 1).

Structure elucidation of these compounds revealed them as quercetin (**1**) [45], gallic acid (**2**) [46], kaempferol (**3**) [46], methyl gallate (**4**), myricetin 3-*O*-α-L-rhamnopyranoside (**5**) [47], (−)-epicatechin-3-*O*-gallate (**6**) [48] and (−)-epigallocatechin-3-*O*-gallate

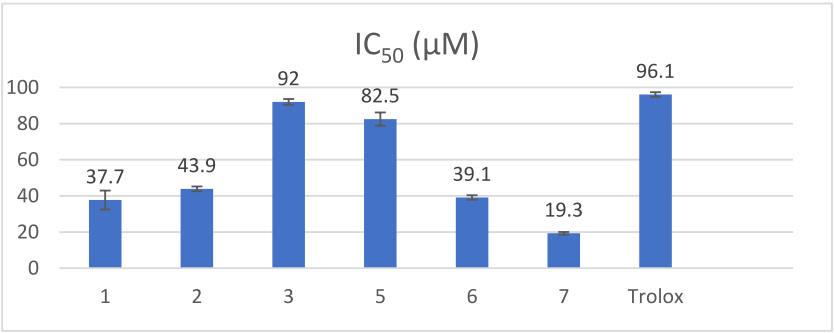

Fig. 2. DPPH scavenging activities (IC_{50} ± SEM: μM) of compounds 1–7 and Trolox. Compound 4 was less potent. Quercetin (1), gallic acid (2), kaempferol (3), methyl gallate (4), myricetin 3-*O*-α-L-rhamnopyranoside (5), (−)-epicatechin-3-*O*-gallate (6) and (−)-epigallocatechin-3-*O*-gallate (7).

(**7**) [49] based on spectroscopic data and comparison with literature. ^{1}H and ^{13}C NMR data and spectra of these compounds are given in Supplementary Materials (Tables S1 and S2 and Fig. S1).

3.2. Invitro antioxidant activity

Antioxidant activity was determined as the ability of isolates to scavenge diphenyl-2-picrylhydrazyl (DPPH) free radical [29]. Compounds **1**, **2**, **3**, **5**, **6,** and **7** were found to be excellent free radical scavengers (Fig. 2).

3.3. Molecular docking analysis

Molecular docking was conducted to provide *in silico* evidence for the in vitro activity and its ethnomedicinal uses and to identify the interactions established with NADPH oxidase and TNF-*α*.

3.4. In silico antioxidant activity

In the active site of target protein NADPH oxidase, the isolated compounds and standard drug (Trolox) were docked within a defined grid. Altogether nine poses were generated for each ligand during ligand-protein interaction. The best poses (ligand with low binding energy (kcal/mol) and low RMSD value), are shown in Fig. 3. The taller the peak (more negative), the lower the binding energy (kcal/mol) and thus the more significant the interaction between ligand and receptor for the antioxidant activity [30,50,51]. Quercetin and (−)-epicatechin-3-*O*-gallate showed the best binding energy (−8.5 kcal/mol) with NADPH oxidase followed by (−)-epigallocatechin-3-*O*-gallate (−8.4 kcal/mol), myricetin 3-*O*-*α*-L-rhamnopyranoside (−8.3 kcal/mol), and kaempferol (−7.9 kcal/mol). The binding energies for the isolated compounds were found to be better as compared to Trolox (−7.6 kcal/mol).

The five isolated compounds with the best binding affinity (low binding energy) compared to Trolox (<−7.6 kcal/mol) were selected to visualize molecular interaction with protein. Co-crystallized ligand (Adenosine-5′-diphosphate) was taken as the reference ligand and it showed hydrogen bonds interaction with AspA179, CysA242, LysA213, TyrA188, LysA187, and ValA214 residues. All the compounds showed at least one hydrogen bond with any of these receptors which may be responsible for the stability of interaction. The active sites were surrounded by IleA160, IleA243, LysA213, AspA179, and ValA214 residues which were involved in almost every interaction. Especially, IleA243 residue was involved in hydrophobic interaction with co-crystallized ligand, standard drug, and all the compounds except for myricetin 3-*O*-*α*-L-rhamnopyranoside (did not show hydrophobic interaction). The interactions of the target with the ligands (isolated and standard) are shown in Fig. 4 ((−)-epicatechin-3-*O*-gallate), Fig. 5 (Trolox) Supplementary S2-5, and Tables S3–4.

3.5. In silico anti-inflammatory activity

In the active site of the target protein: TNF-*α*, the isolates (ligands) were docked within defined grid. Altogether nine poses were generated for each ligand during ligand-protein interaction. The best poses, which is a ligand with low binding energy (kcal/mol) and low RMSD value (0), are shown in Fig. 6. The taller the peak, the lower the binding energy and thus the more significant the interaction between ligand and receptor for the anti-inflammatory activity [31,50,51]. The compound (−)-epicatechin-3-*O*-gallate revealed the best binding affinity at −8.9 kcal/mol followed by (−)-epigallocatechin-3-*O*-gallate (−8.8 kcal/mol), myricetin 3-*O*-*α*-L-rhamnopyranoside (−8.6 kcal/mol), and quercetin (−7.8 kcal/mol). This interaction was better than standard prednisolone (−7.6 kcal/mol) as shown in Fig. 6.

The four isolated compounds with good binding affinity (low binding energy), as compared to prednisolone (<−7.6 kcal/mol),

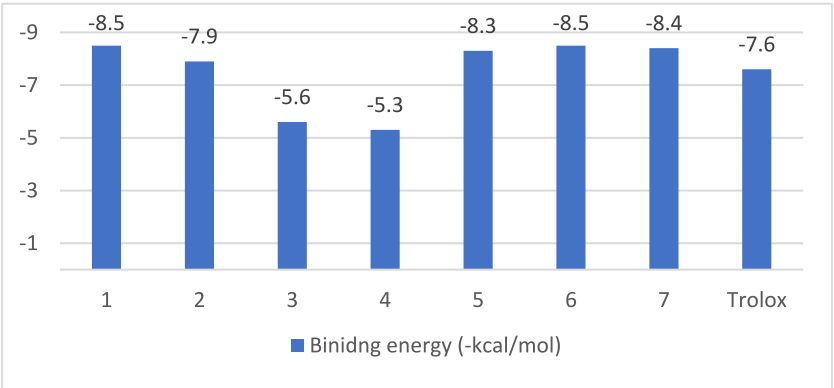

Fig. 3. Binding energies of the seven isolated compounds and Trolox (ligands) with NADPH oxidase (macromolecule/target). Data represented in negative scale. Quercetin (1), gallic acid (2), kaempferol (3), methyl gallate (4), myricetin 3-O-*α*-L-rhamnopyranoside (5), (−)-epicatechin-3-*O*-gallate (6) and (−)-epigallocatechin-3-*O*-gallate (7*)*.

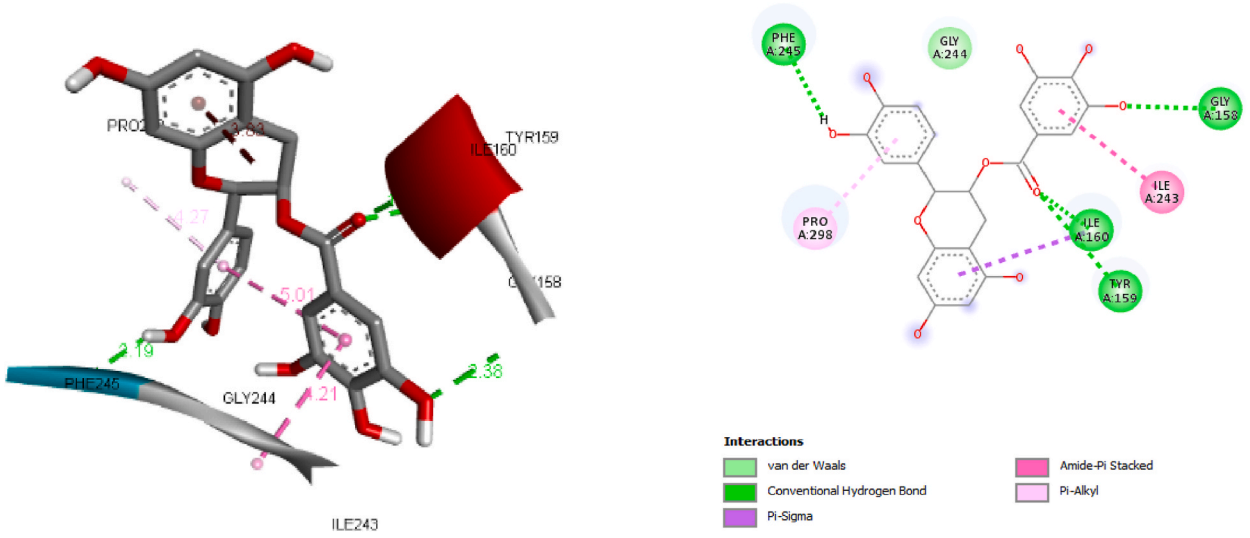

Fig. 4. Interaction of (−)-epicatechin-3-*O*-gallate and NADPH oxidase (3D and 2D interactions).

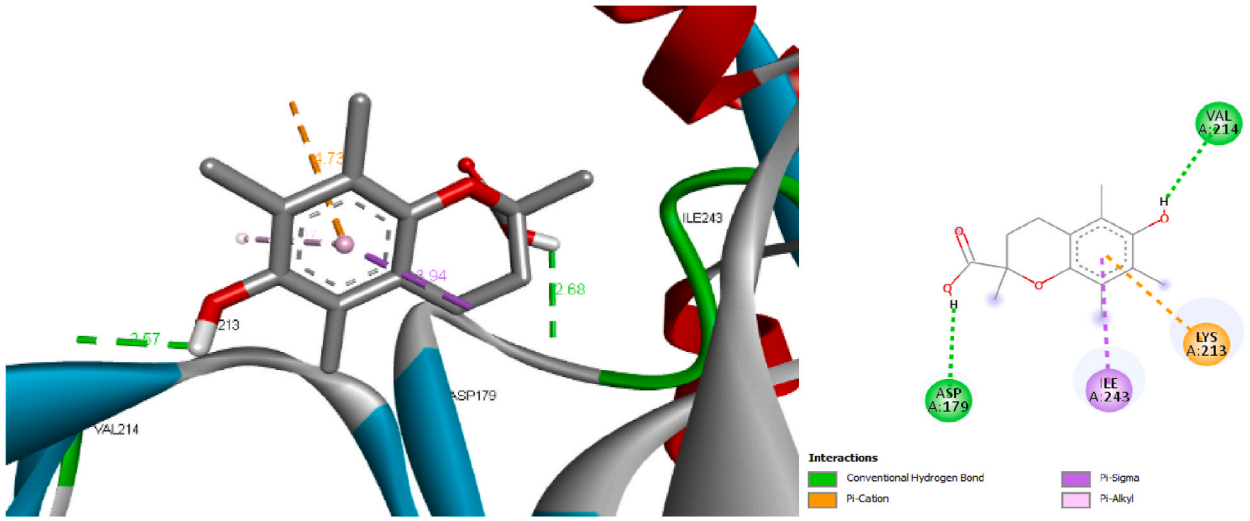

Fig. 5. Interaction of Trolox with NADPH oxidase enzyme (3D and 2D interactions).

were selected to visualize molecular interaction with receptors. Co-crystallized ligand SPD304 was taken as reference ligand which is the inhibitor of TNF-α and the molecular interactions were studied which were important for inhibitory actions. It showed one hydrogen bond (C-H bond) with LeuD15, Hydrophobic interactions are Pi-Pi T-shaped interaction with TyrA119, and Pi-alkyl interaction with TyrB59. Similarly, standard prednisolone showed three conventional hydrogen bonds with TyrB119, TyrB151, and GlyA121. Two Pi-alkyl hydrophobic interactions with TyrB119 and TyrA119 were observed (Fig. 9, Tables S5 and S6). All four isolated compounds and Prednisolone showed strong hydrophobic interactions with TyrA119 and TyrB119 along with the hydrogen bond with TyrB residues similar to co-crystallized ligands. Hydrogen bonds with Ser60 were common for all the isolated compounds. Three Compounds (−) -epicatechin-3-*O*-gallate (Fig. 7), epigallocatechin-3-*O*-gallate (Fig. 8), and myricetin 3-*O*-α-L-rhamnopyranoside (Fig. S6) showed at least one hydrogen bond with Tyr residue. Interactions for the rest of the ligands are provided as supplementary figures (S6-7).

3.6. Molecular docking simulation

To enhance the analysis and ascertain the stability of the docking complexes, we conducted classical MD simulations on epicatechin-3-*O*-gallate in an aqueous environment. This methodology enabled us to explore the dynamic interactions within the ligand-protein complex and evaluate the durability of the binding configuration suggested by the molecular docking investigation. We

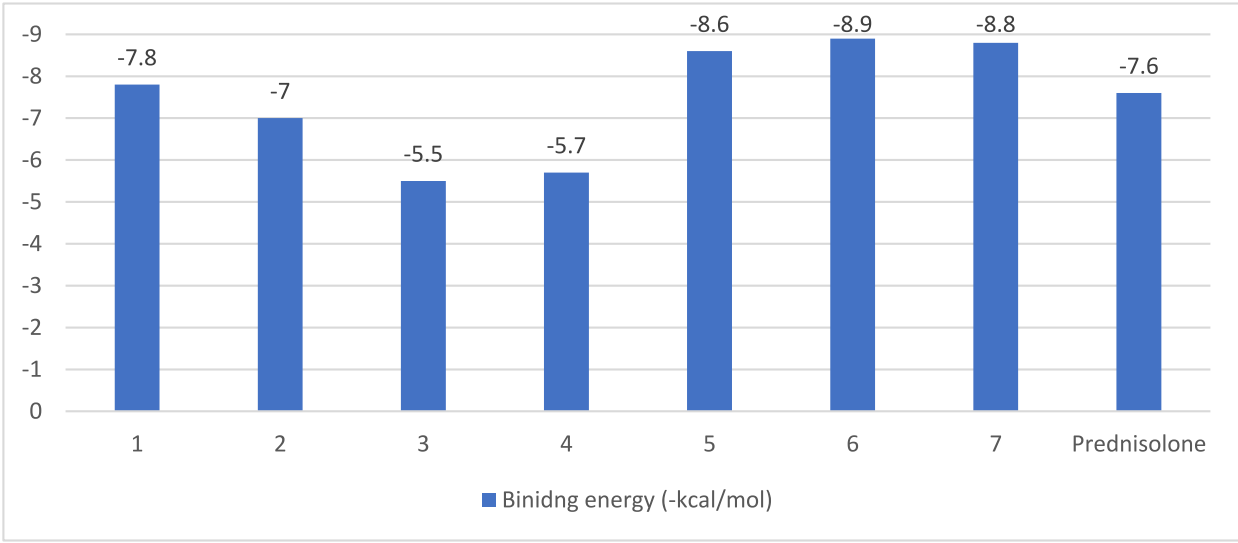

Fig. 6. Binding energy of isolated ligands and Prednisolone with TNF-α. Quercetin (1), gallic acid (2), kaempferol (3), methyl gallate (4), myricetin 3-*O*-α-L-rhamnopyranoside (5), (−)-epicatechin-3-*O*-gallate (6) and (−)-epigallocatechin-3-*O*-gallate (7).

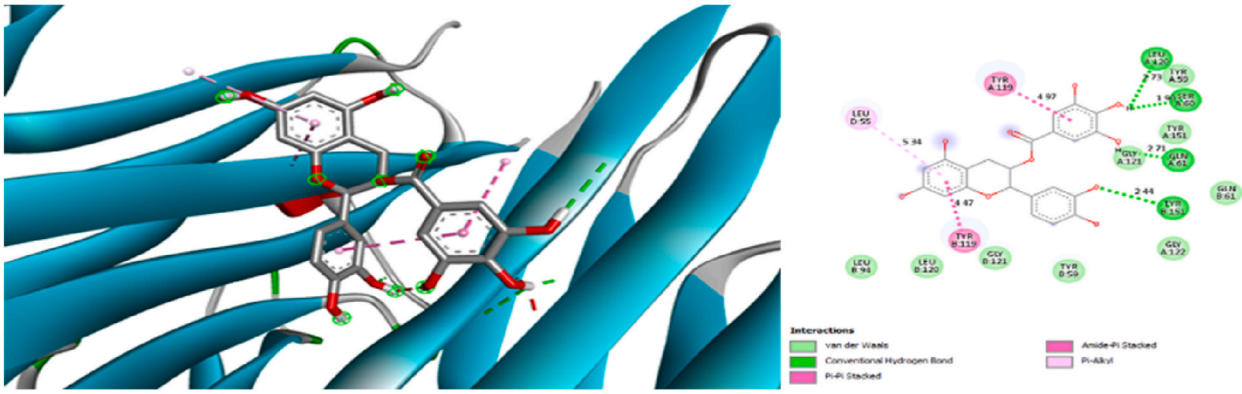

Fig. 7. Interaction of (−)-epicatechin-3-*O*-gallate with TNF- α (3D and 2D interactions).

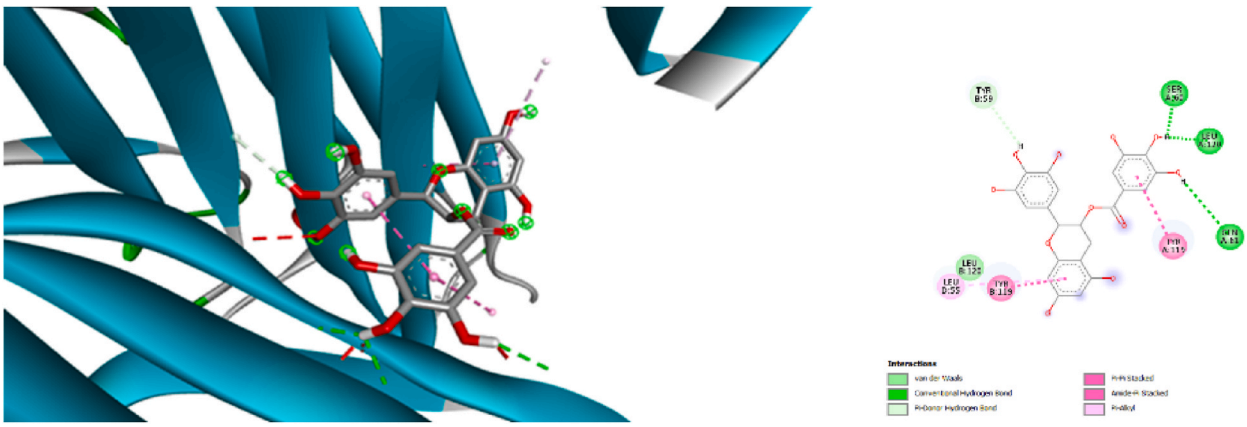

Fig. 8. Interaction of (−)-epigallocatechin-3-*O*-gallate with TNF-α (3D and 2D interactions).

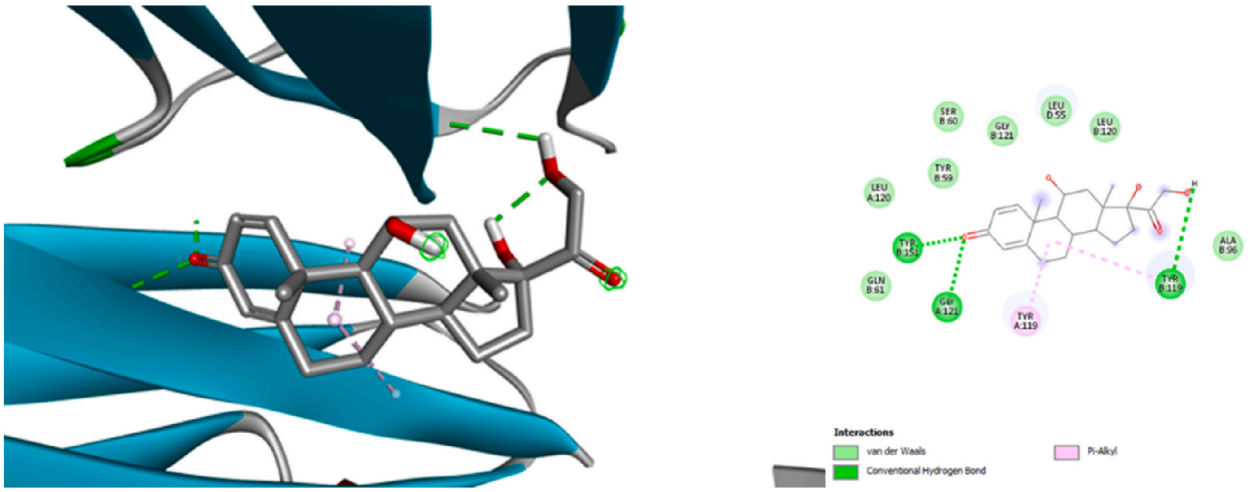

Fig. 9. Interaction of Prednisolone with TNF- α enzyme (3D and 2D interactions).

carefully scrutinized the MD trajectories of all complexes to evaluate stability, structural characteristics, and system convergence throughout the simulation period.

In this context, the overall structural fluctuations and conformational stability of each complex were assessed by analyzing the Root-mean-square deviation (RMSD) of the α-carbon atoms over the simulation time. The RMSD reflects the deviation of atoms within the protein structure throughout the MD simulation. Ideally, the RMSD value of α-carbons in the protein should remain below 3 Å once the system has equilibrated. Higher RMSD values indicate that the system has undergone significant conformational changes. A

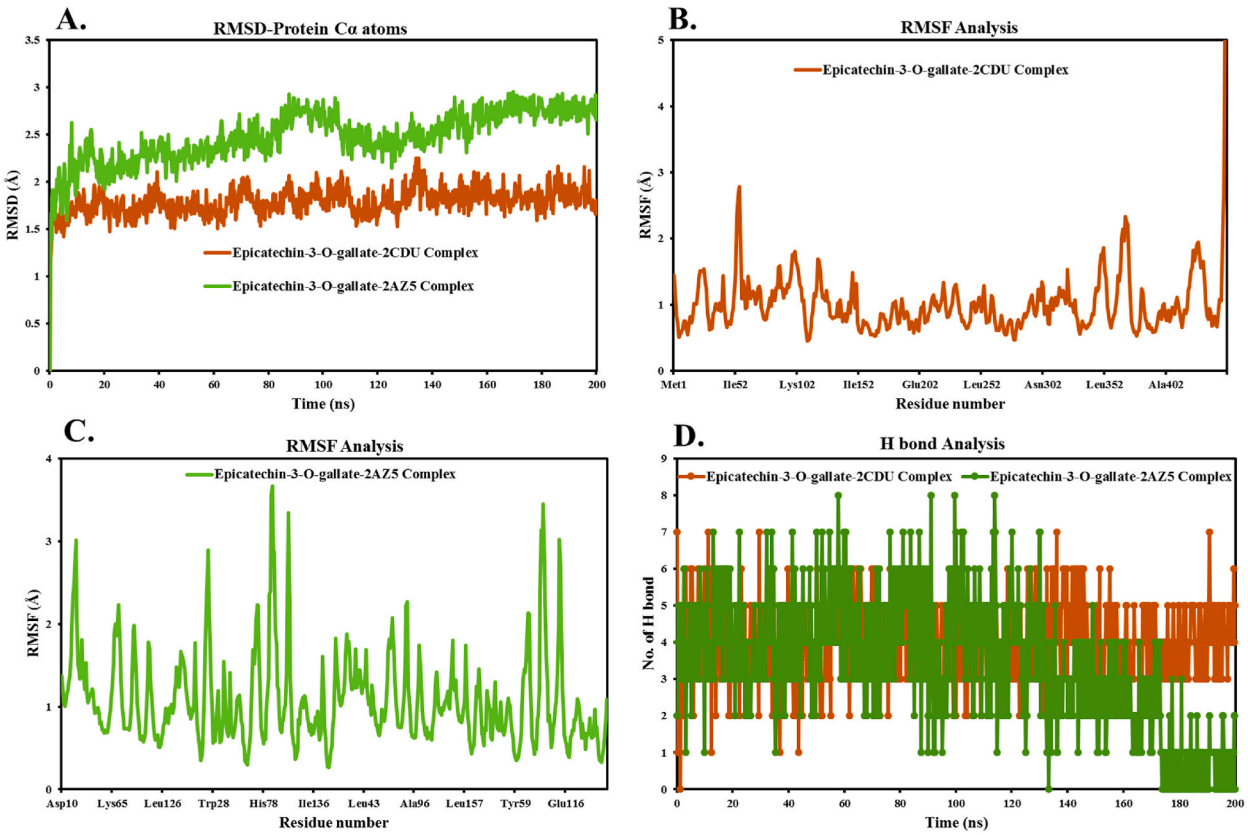

Fig. 10. A. Time-dependent RMSD of 2CDU and 2AZ5 proteins Cα atoms in complex with epicatechin-3-*O*-gallate; B. RMSF of individual amino acids of 2CDU protein; C. RMSF of individual amino acids of 2AZ5 protein; D. Time-dependent Hydrogen Bond analysis of epicatechin-3-*O*-gallate in complex with 2CDU and 2AZ5 proteins.

gradual, steady RMSD slope during the simulation suggests a more stable system, whereas significant fluctuations in the RMSD graph indicate an unstable binding of the ligand to the target protein structure [52–54].

Initially, the RMSD values for both complexes start below 2 Å, indicating a well-optimized initial structure. As the simulation progressed, the RMSD for the epicatechin-3-*O*-gallate-2CDU Complex (orange) remained consistent, reaching around 2.32 Å by 134 ns and fluctuating between 2.2 and 1.5 Å for the remainder of the simulation. Similarly, the epicatechin-3-*O*-gallate-2AZ5 Complex (green) shows an increase in RMSD, stabilizing between 2.0 and 3.0 Å. In this complex, minor fluctuations are observed at 85 ns with RMSD up to 2.89 Å. Both complexes exhibit fluctuations, but they remain within a similar range, indicating a comparable level of stability. The average RMSD values for the α-carbon atoms were observed to be 1.79 Å for the epicatechin-3-*O*-gallate-2CDU Complex and 2.48 Å for the epicatechin-3-*O*-gallate-2AZ5 Complex, respectively (Fig. 10).

3.7. ADME prediction and drug-likeness

SwissADME online tool was used to predict the *in silico* pharmacokinetic properties i.e. Absorption, Distribution, Metabolism, and Elimination, and also to predict Drug-Likeness of the isolates from *Leea asiatica.* This study found that all isolated compounds showed low GI absorption compared to standard trolox. Only two compounds gallic acid and methyl gallate showed GI absorption higher than standard prednisolone. All the compounds indicated the bioavailability and plasma concentration. No compounds crossed the brain blood barrier (BBB). Cytochrome P450 (CYP450) is the major liver enzyme system and hence plays a critical role in drug metabolism. Quercetin and kaempferol behave as CYP1A2, CYP2D6, and CYP3A4 inhibitors and on the other hand, gallic acid behaves as CYP3A4 inhibitors which means they decrease the elimination and metabolism, increasing bioavailability.

The drug-likeness properties of isolated compounds of *Leea asiatica* were evaluated by using SwissADME. The five filters given by Swiss ADME define an active molecule's drug likeness properties including Lipinski, Ghose, Veber, Egan, and Muegge. In our study, the isolated compounds with standard drugs obey all five filters with not exceeding 3 violations. The pharmacokinetic parameters of ADME and drug-likeness are provided as included in supplementary tables (Tables S7–11).

3.8. Evaluation of toxicity

The computational method also can be employed to determine the toxicity of the compounds and help to eliminate unsuitable compounds from the drug screening process. In the current study, the isolated compounds from *Leea asiatica* were employed for toxicity studies such as carcinogenicity, hepatotoxicity, mutagenicity, immunogenicity, and cytotoxicity versus standard drugs by using the ProTox online tool. The compounds quercetin, gallic acid, and myricetin 3-*O*-α-L-rhamnopyranoside show potent carcinogenic effects but quercetin shows both carcinogenic and mutagenic effects (Table S12). The reference prednisolone shows immunogenic effects. The structural modification of isolated compounds can minimize the toxic effects.

4. Discussion

Leea asiatica is reported to have been used to treat eye diseases, diabetes, gastrointestinal disorders, and liver disorders by the ethnic tribes of Asian countries [24]. Several studies report that the methanolic extracts of the plant possess analgesic, anti-inflammatory, hepatoprotective, and nephroprotective properties [25,26], and these conditions share a common pathophysiology of increased oxidative stress and cellular inflammation [55]. The 70 % methanolic extract of the aerial parts of the plant gave 7 major polyphenolic compounds: Quercetin (**1**), gallic acid (**2**), kaempferol (**3**), methyl gallate (**4**), myricetin 3-*O*-α-L-rhamnopyranoside (**5**), (−)-epicatechin-3-*O*-gallate (**6**) and (−)-epigallocatechin-3-*O*-gallate (**7**) of which (**1**), (**3**) and (**5**) have previously been reported from *Leea asiatica* [27,28]. This is the first report of gallic acid (**2**), methyl gallate (**4**), (−)-epicatechin-3-*O*-gallate (**6**) and (−)-epigallocatechin-3-*O*-gallate (**7**) from the plant. All of the isolated compounds were found to be a potent scavenger of DPPH free radicals as compared to Trolox (water soluble analogue of Vitamin E) [56]. The DPPH free radical scavenging potential (an in vitro marker of antioxidant potential) [57] was the greatest for (−)-epigallocatechin-3-*O*-gallate (19.3 μM) followed by quercetin (37.7 μM) and (−)-epicatechin-3-*O*-gallate (39.1 μM).

In the *in silico* antioxidant study, five isolated compounds showed lower binding energy except methyl gallate and gallic acid (also possessed less potent DPPH free radical scavenging activity) in comparison to Trolox. The significance of ligand-receptor interaction increases with decrease in the binding energy (more negative value) [30,50,51]. Quercetin and -(−)-epicatechin-3-*O*-gallate showed better interaction with low binding energy among all the isolated compounds. The molecular interaction study showed ligand interaction with aspartic acid, isoleucine and valine residues (potentially AspA179, IleA243, and ValA214) of NADPH oxidase enzyme were important for the antioxidant activity. This was further supported by the study that reported similar interactions and active sites [30,31]. AspA179 and ValA214 were the TNF-α active residues for hydrogen bond interactions. Ligands were also seen for hydrophobic interaction with AspA179 and IleA243 residues. These hydrogen bonding and hydrophobic interaction with crucial residues of NADPH oxidase are responsible for the stable interaction resulting in the antioxidant activity as NADPH oxidase is responsible for generation of ROS.

The *in silico* anti-inflammatory activity showed -(−)-epicatechin-3-0-gallate has lower binding energy and the binding energy is even lower (more negative) than prednisolone. Molecular interaction with tyrosine residues (potentially Tyr119) was important for the TNF-α inhibition. TyrA119 and TyrB119 were the TNF-α active residues for hydrophobic interactions. Ligands were also seen for hydrogen bond formation with Tyr residues. These findings are similar to ones reported in other studies [31] that report tyrosine residues as the active binding site of TNF-α for inhibition. Of the major compounds isolated from *Leea asiatica,* three compounds

showed hydrogen bond contacts and strong hydrophobic interactions with the crucial residues of the TNF-α.

The Root Mean Square Fluctuation (RMSF) is a crucial metric in molecular dynamics simulations used to assess the average deviation of protein residues from a reference position over time. This metric provides dynamic insights into the behavior of protein structures, shedding light on their flexibility and rigidity. By quantifying these deviations, RMSF offers a detailed view of the fluctuations within different regions of the protein, highlighting areas that exhibit significant variability and those that remain relatively stable throughout the simulation [58–60]. In the context of the study involving the epicatechin-3-*O*-gallate-2CDU and epicatechin-3-*O*-gallate-2AZ5 complexes, the RMSF analysis revealed distinct patterns of fluctuation in different protein residues. The epicatechin-3-*O*-gallate-2CDU complex displayed major RMSF fluctuations in Asn254, Asn255, and the N-terminal residue, indicating significant flexibility in these regions (Fig. 10 B). On the other hand, the epicatechin-3-*O*-gallate-2AZ5 complex showed significant fluctuations in residues such as Thr89, Glu23, Gly24, Arg103, Val85, Tyr87, and Ser86, suggesting dynamic behavior in these areas (Fig. 10C). It was observed that epicatechin-3-*O*-gallate interacts with 2AZ5 protein residues, including Ser60, Tyr119, Leu120, Tyr59, Ile58, Leu120, Tyr119, Gly121, Gly122, Ser60, Ile58, Val123, Gln61, Ser95, Leu57, Gly122, Gly121, Gln125, Leu55, Glu53, Tyr151, Leu157, Lys11, and Gln149, while in 2CDU, Thr9, His10, Leu40, Ser41, Gly43, Ile44, Thr113, Ser115, Cys133, Lys134, Asn135, Gly156, Ser157, Gly158, Tyr159, Ile160, Gly161, Glu163, Asp179, His181, Tyr186, Lys187, Tyr188, Cys242, Ile243, Gly244, Phe245, Arg246, Asn261, Asp282, Tyr296, Pro298, Leu299, Ala300, Thr301, Ser326, Ser327, Ser328, and Gly329. All the interacted residues have RMSF values less than 2 Å, indicating the stability of epicatechin-3-*O*-gallate under dynamic conditions. These interactions were found to exhibit RMSF values of less than 2 Å. This observation indicates that epicatechin-3-*O*-gallate maintains stability within the complex environment, as these residues show minimal deviation from their initial positions during the simulation.

Hydrogen bond analysis in MD simulations is of paramount importance for unraveling the intricate dynamics and interactions within bimolecular systems. These bonds, formed between hydrogen atoms and electronegative atoms like oxygen or nitrogen, play a fundamental role in shaping the structure, stability, and function of proteins [61–63]. Hydrogen bond analysis is essential for understanding molecular interactions within complexes such as those involving epicatechin-3-*O*-gallate with different protein structures. In the case of the epicatechin-3-*O*-gallate-2CDU complex, the number of hydrogen bonds ranges from 1 to 7, with an average of 4.00. This indicates a relatively consistent and stable interaction between epicatechin-3-*O*-gallate and the protein in this complex. Conversely, the epicatechin-3-*O*-gallate-2AZ5 complex exhibits a hydrogen bond range from 1 to 8, but with a much lower average of 1.31. This suggests that while 2AZ5 can form more hydrogen bonds at its maximum, it generally maintains fewer hydrogen bonds on average, indicating moderate interactions (Fig. 10 D). The higher average hydrogen bond count in the 2CDU complex suggests stronger and more stable binding, potentially leading to higher binding affinity and stability.

From the in-silico study, it was found -(−)-epicatechin-3-*O*-gallate, together with other antioxidant compounds might be responsible for the ethnomedicinal property of the plant in the management of inflammatory conditions. Further, -(−)-epicatechin-3-*O*-gallate can be a potential candidate for antioxidant and anti-inflammatory agents as it shows better binding interactions with receptors as compared to standard (Trolox and prednisolone). The MD simulation analysis of epicatechin-3-*O*-gallate complexes with 2CDU and 2AZ5 proteins reveals that the epicatechin-3-*O*-gallate-2CDU complex demonstrates greater stability and stronger interactions, as indicated by lower RMSD and higher average hydrogen bond counts (Fig. 10A). In contrast, the epicatechin-3-*O*-gallate-2AZ5 complex shows moderate interactions and stability, with slightly higher RMSD values and fewer average hydrogen bonds (Fig. 10A). This correlates with the in vitro DPPH free radical scavenging activity where -(−)-epicatechin-3-*O*-gallate shows more than twice the potency compared to Trolox. Swiss ADME study shows low GI absorption in humans compared to standard and structural modification can increase the water solubility of the compound. It follows the drug-likeness properties like Lipinski and Ghose. Toxicity study shows no kind of toxicity for these compounds. In-silico approach provides the information about the predictive mode of action, ADME properties and toxicity of compounds in very short period of time. We used in-silico process to predict the binding mode and their stability. This will help to design the in vitro and in vivo experiments for the isolated compounds.

5. Conclusion

In conclusion, *Leea asiatica* exhibits promising medicinal properties supported by both traditional use and scientific research. The 70 % methanolic extracts of the plant have shown analgesic, anti-inflammatory, hepatoprotective, and nephroprotective properties, attributed to their antioxidant activities. This study identified seven major polyphenolic compounds from the aerial parts of plant, with some reported for the first time, including gallic acid and (−)-epigallocatechin-3-*O*-gallate, which displayed the highest DPPH free radical scavenging activity. In silico studies further demonstrated the strong antioxidant and anti-inflammatory potential of these compounds, particularly (−)-epicatechin-3-*O*-gallate, which showed superior binding interactions compared to standards like Trolox and prednisolone. Molecular dynamics simulations revealed that the epicatechin-3-*O*-gallate-2CDU complex had greater stability and stronger interactions, correlating with in vitro antioxidant activity. These findings emphasize the potential of *Leea asiatica*, especially (−)-epicatechin-3-*O*-gallate, as a candidate for developing antioxidant and anti-inflammatory agents. Future research should focus on structural modifications to enhance bioavailability and further explore the therapeutic applications of these compounds.

Ethical statement

NA.

Funding

NA.

Data availability

Data to support the findings of the current study are available within the article and its supplementary files.

CRediT authorship contribution statement

Khem Raj Joshi: Writing – review & editing, Writing – original draft, Methodology, Investigation. **Hari Prasad Devkota:** Writing – review & editing, Methodology, Formal analysis. **Khalid Awadh Al-Mutairi:** Writing – original draft. **Koji Sugimura:** Writing – review & editing. **Shoji Yahara:** Supervision, Conceptualization. **Ravindra Khadka:** Software, Methodology, Data curation. **Shankar Thapa:** Writing – original draft. **Mohammad Ujair Shekh:** Validation, Data curation. **Sandesh Poudel:** Writing – review & editing, Data curation. **Takashi Watanabe:** Writing – review & editing, Conceptualization.

Declaration of competing interest

The authors declare that they have no known competing financial interests or personal relationships that could have appeared to influence the work reported in this paper.

Acknowledgements

The authors extend their gratitude to the Ministry of Education, Culture, Sports, Science, and Technology (MEXT) of Japan for granting the PhD scholarship to Khem Raj Joshi.

Appendix A. Supplementary data

Supplementary data to this article can be found online at https://doi.org/10.1016/j.heliyon.2024.e38074.

References

[1] A. Amaral Da Silva, Reactive oxygen species and the respiratory tract diseases of large animals. https://www.researchgate.net/publication/226771659, 2014.
[2] J. Yun, E. Mullarky, C. Lu, K.N. Bosch, A. Kavalier, K. Rivera, J. Roper, I.I.C. Chio, E.G. Giannopoulou, C. Rago, A. Muley, J.M. Asara, J. Paik, O. Elemento, Z. Chen, D.J. Pappin, L.E. Dow, N. Papadopoulos, S.S. Gross, L.C. Cantley, Vitamin C selectively kills KRAS and BRAF mutant colorectal cancer cells by targeting GAPDH, Science (1979) 350 (2015) 1391–1396, https://doi.org/10.1126/science.aaa5004.
[3] P.A.S. White, R.C.M. Oliveira, A.P. Oliveira, M.R. Serafini, A.A.S. Araújo, D.P. Gelain, J.C.F. Moreira, J.R.G.S. Almeida, J.S.S. Quintans, L.J. Quintans-Junior, M. R.V. Santos, Antioxidant activity and mechanisms of action of natural compounds isolated from lichens: a systematic review, Molecules 19 (2014) 14496–14527, https://doi.org/10.3390/molecules190914496.
[4] S. Reuter, S.C. Gupta, M.M. Chaturvedi, B.B. Aggarwal, Oxidative stress, inflammation, and cancer: how are they linked? Free Radic. Biol. Med. 49 (2010) 1603–1616, https://doi.org/10.1016/j.freeradbiomed.2010.09.006.
[5] E. Cadenas, Basic Mechanisms of Antioxidant Activity, 1997.
[6] A.T. Dharmaraja, Role of reactive oxygen species (ROS) in therapeutics and drug resistance in cancer and bacteria, J. Med. Chem. 60 (2017) 3221–3240, https://doi.org/10.1021/acs.jmedchem.6b01243.
[7] L. Aljerf, M. Williams, A.B. Ajong, U.P. Onydinma, F. Dehmchi, V.T. Pham, S. Bhatnagar, N. Belboukhari, Comparative study of the biochemical response behavior of some highly toxic minerals on selenosis in rats, Rev Chim 72 (2021) 9–18.
[8] S.L. Montgomery, W.J. Bowers, Tumor necrosis factor-alpha and the roles it plays in homeostatic and degenerative processes within the central nervous system, J. Neuroimmune Pharmacol. 7 (2012) 42–59, https://doi.org/10.1007/s11481-011-9287-2.
[9] B.B. Aggarwal, S.C. Gupta, J.H. Kim, Historical perspectives on tumor necrosis factor and its superfamily: 25 years later, a golden journey, Blood 119 (2012) 651–665, https://doi.org/10.1182/blood-2011-04-325225.
[10] S. Yang, J. Wang, D.D. Brand, S.G. Zheng, Role of TNF-TNF receptor 2 signal in regulatory T cells and its therapeutic implications, Front. Immunol. 9 (2018), https://doi.org/10.3389/fimmu.2018.00784.
[11] K. Urschel, I. Cicha, TNF-α in the cardiovascular system: from physiology to therapy, Int. J. Interferon Cytokine Mediat. Res. 7 (2015) 9–25, https://doi.org/10.2147/IJICMR.S64894.
[12] M. Feldmann, R.N. Maini, TNF defined as a therapeutic target for rheumatoid arthritis and other autoimmune diseases. http://www.nature.com/naturemedicine, 2003.
[13] M. Ángel Gonzalez-Gay, C. Gonzalez-Juanatey, J. Martin, Influence of anti-TNF-alpha infliximab therapy on adhesion molecules associated with atherogenesis in patients with rheumatoid arthritis. https://www.researchgate.net/publication/6834741, 2014.
[14] S. Madhusudan, M. Foster, S.R. Muthuramalingam, J.P. Braybrooke, S. Wilner, K. Kaur, C. Han, S. Hoare, F. Balkwill, D.C. Talbot, T.S. Ganesan, A.L. Harris, A Phase II Study of Etanercept (Enbrel), a Tumor Necrosis Factor Inhibitor in Patients with Metastatic Breast Cancer, 2004.
[15] P. Neri, M. Zucchi, P. Allegri, M. Lettieri, C. Mariotti, A. Giovannini, Adalimumab (Humira™): a promising monoclonal anti-tumor necrosis factor alpha in ophthalmology, Int. Ophthalmol. 31 (2011) 165–173, https://doi.org/10.1007/s10792-011-9430-3.
[16] P. Kawalec, A. Mikrut, N. Wiśniewska, A. Pilc, Tumor necrosis factor-α antibodies (infliximab, adalimumab and certolizumab) in Crohn's disease: systematic review and meta-analysis, Arch. Med. Sci. 9 (2013) 765–779, https://doi.org/10.5114/aoms.2013.38670.
[17] H. Zhou, H. Jang, R.M. Fleischmann, E. Bouman-Thio, Z. Xu, J.C. Marini, C. Pendley, Q. Jiao, G. Shankar, S.J. Marciniak, S.B. Cohen, M.U. Rahman, D. Baker, M. A. Mascelli, H.M. Davis, D.E. Everitt, Pharmacokinetics and safety of golimumab, a fully human anti-TNF-α monoclonal antibody, in subjects with rheumatoid arthritis, J. Clin. Pharmacol. 47 (2007) 383–396, https://doi.org/10.1177/0091270006298188.

[18] W.G. Dixon, K.L. Hyrich, K.D. Watson, M. Lunt, J. Galloway, A. Ustianowski, D.P.M. Symmons, Drug-specific risk of tuberculosis in patients with rheumatoid arthritis treated with anti-TNF therapy: results from the British Society for Rheumatology Biologics Register (BSRBR), Ann. Rheum. Dis. 69 (2010) 522–528, https://doi.org/10.1136/ard.2009.118935.

[19] M. Debandt, O. Vittecoq, V. Descamps, X. Le Loët, O. Meyer, Anti-TNF-α-induced systemic lupus syndrome, Clin. Rheumatol. 22 (2003) 56–61, https://doi.org/10.1007/s10067-002-0654-5.

[20] N. Mohan, E.T. Edwards, T.R. Cupps, P.J. Oliverio, G. Sandberg, H. Crayton, J.R. Richert, J.N. Siegel, Demyelination Occurring during Anti-tumor Necrosis Factor Therapy for Inflammatory Arthritides, 2001.

[21] N. Scheinfeld, A comprehensive review and evaluation of the side effects of the tumor necrosis factor alpha blockers etanercept, infliximab and adalimumab, J. Dermatol. Treat. 15 (2004) 280–294, https://doi.org/10.1080/09546630410017275.

[22] M.M. He, A.S. Smith, J.D. Oslob, W.M. Flanagan, A.C. Braisted, A. Whitty, M.T. Cancilla, J. Wang, A.A. Lugovskoy, J.C. Yoburn, A.D. Fung, G. Farrington, J.K. Eldredge, E.S. Day, L.A. Cruz, T.G. Cachero, S.K. Miller, J.E. Friedman, I.C. Choong, B.C. Cunningham, Small-Molecule Inhibition of TNF-a, n.d. www.sciencemag.org.

[23] M. Gupta, R. Sharma, A. Kumar, Docking techniques in pharmacology: how much promising? Comput. Biol. Chem. 76 (2018) 210–217, https://doi.org/10.1016/j.compbiolchem.2018.06.005.

[24] F. Hossain, M.G. Mostofa, A.K. Alam, Traditional uses and pharmacological activities of the genus leea and its phytochemicals: a review, Heliyon 7 (2021) e06222, https://doi.org/10.1016/j.heliyon.2021.e06222.

[25] S. Sen, B. De, N. Devanna, R. Chakraborty, Cisplatin-induced nephrotoxicity in mice: protective role of Leea asiatica leaves, Ren. Fail. 35 (2013) 1412–1417, https://doi.org/10.3109/0886022X.2013.829405.

[26] S. Sen, B. De, N. Devanna, R. Chakraborty, Hepatoprotective and antioxidant activity of Leea asiatica leaves against acetaminophen-induced hepatotoxicity in rats, TANG [HUMANITAS MEDICINE] 4 (2014) 18.1–18.5, https://doi.org/10.5667/tang.2014.0005.

[27] H.W. Kil, T. Rho, K.D. Yoon, Phytochemical study of aerial parts of leea asiatica, Molecules 24 (2019), https://doi.org/10.3390/molecules24091733.

[28] J. Yang, T. Huang, J. Luo, H. Li, Y. Wang, Chemical constituents from leea asiatica, Natural Product Research and Development 30 (2018) 1382–1386, https://doi.org/10.16333/j.1001-6880.2018.8.016.

[29] L. Li, N.P. Seeram, Further investigation into maple syrup yields 3 new Lignans, a new phenylpropanoid, and 26 other phytochemicals, J. Agric. Food Chem. (2011) 7708–7716, https://doi.org/10.1021/jf2011613.

[30] J. Da Silva Costa, R. Da Silva Ramos, K. Da Silva Lopes Costa, D. Do Socorro Barros Brasil, C.H.T. De Paula Da Silva, E.F.B. Ferreira, R. Dos Santos Borges, J. M. Campos, W.J. Da Cruz Macêdo, C.B.R. Dos Santos, An in silico study of the antioxidant ability for two caffeine analogs using molecular docking and quantum chemical methods, Molecules 23 (2018), https://doi.org/10.3390/molecules23112801.

[31] K. Zia, S. Ashraf, A. Jabeen, M. Saeed, M. Nur-e-Alam, S. Ahmed, A.J. Al-Rehaily, Z. Ul-Haq, Identification of potential TNF-α inhibitors: from in silico to in vitro studies, Sci. Rep. 10 (2020), https://doi.org/10.1038/s41598-020-77750-3.

[32] G.T. Lountos, R. Jiang, W.B. Wellborn, T.L. Thaler, A.S. Bommarius, A.M. Orville, The crystal structure of NAD(P)H oxidase from Lactobacillus sanfranciscensis: insights into the conversion of O2 into two water molecules by the flavoenzyme, Biochemistry 45 (2006) 9648–9659, https://doi.org/10.1021/BI060692P.

[33] S. Thapa, S.L. Nargund, M.S. Biradar, Molecular design and in-silico analysis of trisubstituted benzimidazole derivatives as Ftsz inhibitor, J. Chem. 2023 (2023), https://doi.org/10.1155/2023/9307613.

[34] B. Shaker, M.S. Yu, J. Lee, Y. Lee, C. Jung, D. Na, User guide for the discovery of potential drugs via protein structure prediction and ligand docking simulation, J. Microbiol. 58 (2020) 235–244, https://doi.org/10.1007/s12275-020-9563-z.

[35] S. Dallakyan, A.J. Olson, Small-molecule library screening by docking with PyRx, Methods Mol. Biol. 1263 (2015) 243–250, https://doi.org/10.1007/978-1-4939-2269-7_19.

[36] O. Trott, A.J. Olson, AutoDock Vina: improving the speed and accuracy of docking with a new scoring function, efficient optimization, and multithreading, J. Comput. Chem. 31 (2010) 455–461, https://doi.org/10.1002/jcc.21334.

[37] N.M. O'Boyle, M. Banck, C.A. James, C. Morley, T. Vandermeersch, G.R. Hutchison, Open babel: an open chemical toolbox, J. Cheminf. 3 (2011), https://doi.org/10.1186/1758-2946-3-33.

[38] A.M. Metwaly, A. Elwan, A.A.M.M. El-Attar, S.T. Al-Rashood, I.H. Eissa, Structure-based virtual screening, docking, ADMET, molecular dynamics, and MM-PBSA calculations for the discovery of potential natural SARS-CoV-2 helicase inhibitors from the traditional Chinese medicine, J. Chem. 2022 (2022), https://doi.org/10.1155/2022/7270094.

[39] L. Pant, S. Thapa, B. Dahal, R. Khadka, M.S. Biradar, In silico and in vitro studies of antibacterial activity of cow urine distillate (CUD), Evid. base Compl. Alternative Med. 2024 (2024) 1–10, https://doi.org/10.1155/2024/1904763.

[40] S. Thapa, S.L. Nargund, M.S. Biradar, J. Banerjee, D. Karati, In-silico investigation and drug likeliness studies of benzimidazole congeners: the new face of innovation, Inform. Med. Unlocked 38 (2023), https://doi.org/10.1016/j.imu.2023.101213.

[41] R. Pawara, I. Ahmad, S. Surana, H. Patel, Computational identification of 2,4-disubstituted amino-pyrimidines as L858R/T790M-EGFR double mutant inhibitors using pharmacophore mapping, molecular docking, binding free energy calculation, DFT study and molecular dynamic simulation, in: Silico Pharmacol, vol. 9, 2021, https://doi.org/10.1007/S40203-021-00113-X.

[42] R. Girase, I. Ahmad, R. Pawara, H. Patel, Optimizing cardio, hepato and phospholipidosis toxicity of the Bedaquiline by chemoinformatics and molecular modelling approach, SAR QSAR Environ. Res. 33 (2022) 215–235, https://doi.org/10.1080/1062936X.2022.2041724.

[43] A. Daina, O. Michielin, V. Zoete, SwissADME: a free web tool to evaluate pharmacokinetics, drug-likeness and medicinal chemistry friendliness of small molecules, Sci. Rep. 7 (2017), https://doi.org/10.1038/srep42717.

[44] P. Banerjee, A.O. Eckert, A.K. Schrey, R. Preissner, ProTox-II: a webserver for the prediction of toxicity of chemicals, Nucleic Acids Res. 46 (2018) W257–W263, https://doi.org/10.1093/nar/gky318.

[45] M.G. Boersma, J. Vervoort, H. Szymusiak, K. Lemanska, B. Tyrakowska, N. Cenas, J. Segura-Aguilar, I.M.C.M. Rietjens, Regioselectivity and reversibility of the glutathione conjugation of quercetin quinone methide, Chem. Res. Toxicol. 13 (2000) 185–191, https://doi.org/10.1021/tx990161k.

[46] J.B. Harborne, T.J. Mabry, The Flavonoids: Advances in Research, Springer, 1982.

[47] X.-N. Zhong, H. Otsuka, T. Ide, E. Hirata, A. Takushi~, Y. Takedā, Three flavonol glycosides from leaves of Myrszne SEC UINII, 1997.

[48] M. Watanabe, Catechins as Antioxidants from Buckwheat (Fagopyrum Esculentum Moench) Groats, 1998.

[49] D. Adrienne L, Ya Cai, Alan P. Davies, J.R. Lewis, 1H and 13C NMR assignments of some green tea polyphenols, Magn. Reson. Chem. 34 (1996) 887–890, https://doi.org/10.1002/(SICI)1097-458X(199611)34:11<887::AID-OMR995>3.0.CO;2-U.

[50] P.L. Kastritis, A.M.J.J. Bonvin, On the binding affinity of macromolecular interactions: daring to ask why proteins interact, J. R. Soc. Interface 10 (2013), https://doi.org/10.1098/rsif.2012.0835.

[51] B.E. Eaton, L. Gold, D.A. Zichi, Let's get specific: the relationship between specificity and affinity, Chem. Biol. 2 (1995) 633–638.

[52] K.K. Bharadwaj, I. Ahmad, S. Pati, A. Ghosh, T. Sarkar, B. Rabha, H. Patel, D. Baishya, H.A. Edinur, Z. Abdul Kari, M.R. Ahmad Mohd Zain, W.I. Wan Rosli, Potent bioactive compounds from seaweed waste to combat cancer through bioinformatics investigation, Front. Nutr. 9 (2022), https://doi.org/10.3389/FNUT.2022.889276.

[53] I. Ahmad, S.R. Akand, M. Shaikh, R. Pawara, S.N. Manjula, H. Patel, Synthesis, molecular modelling study of the methaqualone analogues as anti-convulsant agent with improved cognition activity and minimized neurotoxicity, J. Mol. Struct. 1251 (2022), https://doi.org/10.1016/J.MOLSTRUC.2021.131972.

[54] R. Pawara, I. Ahmad, D. Nayak, S. Wagh, A. Wadkar, A. Ansari, S. Belamkar, S. Surana, C. Nath Kundu, C. Patil, H. Patel, Novel, selective acrylamide linked quinazolines for the treatment of double mutant EGFR-L858R/T790M Non-Small-Cell lung cancer (NSCLC), Bioorg. Chem. 115 (2021), https://doi.org/10.1016/J.BIOORG.2021.105234.

[55] G. Pizzino, N. Irrera, M. Cucinotta, G. Pallio, F. Mannino, V. Arcoraci, F. Squadrito, D. Altavilla, A. Bitto, Oxidative stress: harms and benefits for human health, Oxid. Med. Cell. Longev. 2017 (2017), https://doi.org/10.1155/2017/8416763.

[56] V.F. Sagach, M. Scrosati, J. Fielding, G. Rossoni, C. Galli, F. Visioli, The water-soluble vitamin E analogue Trolox protects against ischaemia/reperfusion damage in vitro and ex vivo. A comparison with vitamin E, Pharmacol. Res. 45 (2002) 435–439, https://doi.org/10.1006/phrs.2002.0993.
[57] M. Agrawal, S. Bansal, K. Chopra, Evaluation of the in vitro and in vivo antioxidant potentials of food grade Phycocyanin, J. Food Sci. Technol. 58 (2021) 4382–4390, https://doi.org/10.1007/s13197-020-04922-4.
[58] S. Ghosh, S. Das, I. Ahmad, H. Patel, In silico validation of anti-viral drugs obtained from marine sources as a potential target against SARS-CoV-2 Mpro, J. Indian Chem. Soc. 98 (2021) 100272, https://doi.org/10.1016/J.JICS.2021.100272.
[59] U. Acar Çevik, I. Celik, A. Işık, I. Ahmad, H. Patel, Y. Özkay, Z.A. Kaplancıklı, Design, synthesis, molecular modeling, DFT, ADME and biological evaluation studies of some new 1,3,4-oxadiazole linked benzimidazoles as anticancer agents and aromatase inhibitors, J. Biomol. Struct. Dyn. 41 (2023) 1944–1958, https://doi.org/10.1080/07391102.2022.2025906.
[60] S. Ghannay, B.S. Aldhafeeri, I. Ahmad, A.E.A.E. Albadri, H. Patel, A. Kadri, K. Aouadi, Identification of dual-target isoxazolidine-isatin hybrids with antidiabetic potential: design, synthesis, in vitro and multiscale molecular modeling approaches, Heliyon 10 (2024) e25911, https://doi.org/10.1016/J.HELIYON.2024.E25911.
[61] Q.A.H. Jaber, A.H. Shentaif, M. Almajidi, I. Ahmad, H. Patel, A.K. Azad, S.M. Alnasser, H.A. Alatawi, F. Menaa, S.Y.M. Alfaifi, M.M. Rahman, M.M. Ali, S.J. A. Rao, Synthesis, structure, and in vitro pharmacological evaluation of some new pyrimidine-2-sulfonamide derivatives and their molecular docking studies on human estrogen receptor alpha and CDK2/cyclin proteins, Russ. J. Bioorg. Chem. 49 (2023) S106–S118, https://doi.org/10.1134/S1068162023080095/METRICS.
[62] H.I. Soni, N.B. Patel, I. Ahmad, H. Patel, G. Rivera, Synthesis, biological evaluation, and in silico molecular docking of N-(4-(4-substitutedphenyl)-6-(substituted aryl) pyrimidin-2-yl)-2-(2-isonicotinoyl hydrazinyl) acetamide, J. Biochem. Mol. Toxicol. 38 (2024) e23634, https://doi.org/10.1002/JBT.23634.
[63] S. Thapa, M.S. Biradar, S.L. Nargund, I. Ahmad, M. Agrawal, H. Patel, A. Lamsal, Synthesis, molecular docking, molecular dynamic simulation studies, and antitubercular activity evaluation of substituted benzimidazole derivatives, Adv Pharmacol Pharm Sci 2024 (2024) 9986613, https://doi.org/10.1155/2024/9986613.